JOURNAL OF THERMOPHYSICS AND HEAT TRANSFER
Vol. 20, No. 1, January–March 2006

Prediction of Gross Parameters During Enclosed Incineration of Energetic Materials

Robert Boehm*
University of Nevada, Las Vegas, Las Vegas, Nevada 89154-4027
Jennifer Politano†
Bechtel-Nevada, North Las Vegas, Nevada 89193
and
Zoran Stefanoski‡
NVIDIA Corporation, Santa Clara, California 95050

A computational technique that can be used to predict the transient air temperature and pressure response when rocket propellant or other energetic material is incinerated in an enclosed space is described. An energy balance is used with details of the heat transfer to the wall of the enclosure. This approach has been applied to estimate transient pressure and temperature response for two series of incinerations at the Nevada Test Site. These tests were performed to dispose of outmoded solid rocket propellant, and they were performed in a sealed-off underground chamber. Results of the model correlate quite well with the experimental data considering the very complicated phenomena that are taking place.

Nomenclature

A	=	surface area of chamber
a, b, c	=	constants
C	=	natural convection correlation constant
Gr	=	Grashoff number
g	=	gravity
H	=	heating value
h	=	enthalpy
$\bar{h}$	=	heat-transfer coefficient
i	=	time-step constant
k	=	thermal conductivity
L	=	length
m	=	mass
P	=	chamber pressure
Pr	=	Prandtl number
Q	=	energy liberated
$\dot{Q}$	=	heat-transfer rate
R	=	ideal-gas constant
T	=	temperature
t	=	time
u	=	internal energy
V	=	volume of chamber
α	=	thermal diffusivity
β	=	coefficient of thermal expansion
γ	=	kinematic viscosity
τ	=	variable of integration

Subscripts

a, air	=	air contents
chamber	=	refers to the amount in the chamber
energetic	=	energetic material contents
i	=	incoming
liberated	=	amount liberated
surface	=	value on the wall surface
total	=	total contribution
wall	=	to the chamber wall
1, 2	=	first and second states

Received 23 November 2004; revision received 3 March 2005; accepted for publication 3 March 2005.

*Distinguished Professor of Mechanical Engineering.
†Senior Engineer.
‡Senior Mechanical/Thermal Engineer, Thermal Engineering Department.

Introduction

As the world's collection of rockets and other weapons age, there is a need to remove selectively the danger that some of these items pose in storage. Several approaches have been proposed to handle this disposal. Problems of removing outmoded energetic munitions and propellants are being faced around the world. There is no standardized method of treatment of these materials; the mode of processing varies widely.

Hermann[1] described a method that can be used for chemical reprocessing of outmoded trinitrotoluene (TNT). After this reprocessing is accomplished, the products can be disposed of in a safe and ecologically favorable manner. General processing of munitions and TNT is discussed, with incineration then following the preliminary processing.

Zhang and Wang[2] have examined the various ways of disposing of explosives and propellants. They considered incineration, as well as physical and chemical processing. In some situations, the various components can be removed to serve a useful service in other applications. When the amount of explosive is small, it is preferred that it be exploded, as this releases smaller amounts of oxides of nitrogen than does incineration. They point out that certain types of explosives and propellants might be appropriate to use as fuel supplements in power plants. It is often the case that the material to be destroyed is dissolved first in a solvent. Both the solvent and the material of interest can then be incinerated. Solvent extraction can also be used to retrieve one or more components from single-stage rocket propellants. Components like nitrocellulose or aluminum powder, if present, can be extracted in this manner. In some cases, differential melting of components might be used to remove one or more components of interest. Chemical reactions can also be used to form components that might have further value.

A base hydrolysis treatment for manufacturing wastes of solid rocket propellant was reported by Borcherding.[3] Details of this chemical treatment, which can be used as an alternative to open burning, were outlined. Minimal emissions are reported using this approach.

Hughes et al.[4] report on a study of open burning of NISIH AA-2 propellant. A model was developed to allow more detailed examination of the incineration processes.

Underwater burning of heterogeneous propellants was described by Vetlicky and Chladek.[5] It was indicated that this approach offered an inexpensive and environmentally desirable approach to the disposal of the propellants considered. Both ammonia and chlorine emissions were greatly decreased from open burning situations.

One approach to the design of munitions is to consider the ultimate disposal of unused items. There have been limited reports of life-cycle planning of munitions' systems. In this approach, not only are the manufacturing, storage, and application considered in the design process, but also disposal or recycling of the material at the end of its useful life. Cumming and Paul[6] described considerations of the life cycle of energetic munitions. Apparently little concern for life-cycle aspects is actually used in product development in the industry.

Demilitarization efforts as well as aging/safety concerns have increased the interest in disposal of various types of ordnance and rocket propellant by incineration. Often this is performed in the open atmosphere. However, this can add undesirable components to the ambient air.

One way to address this potentially undesirable outcome is to burn the energetic material in a closed chamber. The products of the combustion can then be collected and cleaned in an appropriate manner. This approach was the basis of several tests carried out at the Nevada Test Site by the U.S. Department of Defense and the U.S. Department of Energy during the past several years.

Questions that arise during the closed burning of these types of materials involve what peak pressures will be achieved and how long a delay after the initiation of combustion is required to achieve certain appropriate thermal conditions within the chamber. The first of these parameters might be needed to assess the strength requirements of the weakest part of the chamber. The second might be required to know when the product gases have dropped in temperature sufficiently to accomplish a required task, such as gas treatment or for access into the chamber. An approach to these types of predictions is given in what follows.

Analysis

Clearly the combustion of energetic materials in an enclosure is a complicated physical phenomenon. A variety of components, chemical species, enclosures, ignition sources, and pressure and temperature histories make this an almost impossible situation to simulate in a general sense. Our approach is to assume a simplified model based on an energy balance with a representation of heat transfer to the wall.

To gain insight into the elements of the analysis, consider Fig. 1, which shows the system. Any shape of chamber that is characterized by a volume V and a surface area A can be analyzed. It is further assumed that prior to the incineration process the chamber is filled with atmospheric air as well as the item(s) to be combusted. The energetic material is characterized by the active element mass and heat of combustion. It is presumed that after the material is burned all gases (both the initial air and the products of combustion) remain in the chamber.

The initial process is the combustion of the energetic material that is assumed to occur in a nearly instantaneous manner. When this occurs, both heat and mass are added to the air of the chamber.

$$Q_{\text{liberated}} = m_{\text{energetic}} H \tag{1}$$

$$m_{\text{total}} = m_{\text{energetic}} + m_{\text{air}} \tag{2}$$

Analysis of the effect of this addition of heat to the chamber is performed using transient thermodynamic concepts. The products of combustion are assumed to be equivalent to the flow of gas into the chamber. This is shown in Eq. (3):

$$Q_{\text{liberated}} + m_{\text{energetic}} h_i = (m_{\text{total}} u_2 - m_{\text{air}} u_1) \tag{3}$$

This allows the temperature in the chamber following the combustion process to be determined. It is assumed that all of the liberated energy is added directly to the chamber gases. Any transfer of heat

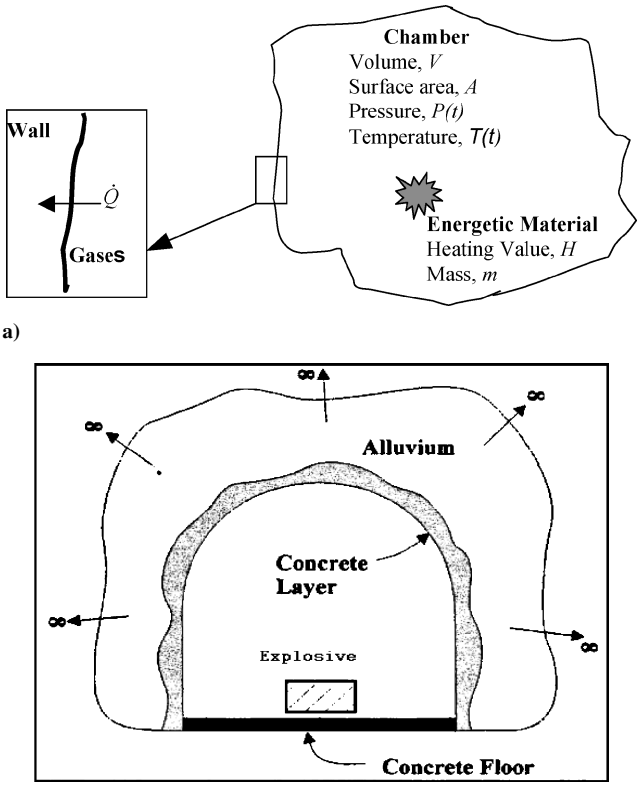

Fig. 1 System considered a) conceptual approach is shown, and b) the lower part of the figure is the system analyzed specifically in this work.

to the walls by radiation has been neglected. This is a good approximation if the combustion process generates a significant amount of smoke. It is further assumed that the air and products of combustion are well mixed by the turbulence caused by the combustion process. Finally, the temperature for the enthalpy of the products of combustion is taken to be at the adiabatic flame value of the energetic material. The value u_2 is used to find the maximum temperature in the chamber that is assumed to exist at the completion of the combustion process.

Both the air and the mixture of air and products of combustion are treated as ideal gases with the properties of air. If pressures approaching about 50% of the critical pressure of air are encountered, this might not be a good assumption. The ideal gas assumption applies quite well for the current study. Hence the gas pressure in the chamber at any time can be represented by

$$P_{\text{chamber}} = m_{\text{total}} R T_{\text{chamber}} / V_{\text{chamber}} \tag{4}$$

With the temperature dictating the value of the pressure, the steps involved in the calculation of the temperature are important. We will apply an energy balance on the air that is influenced greatly by wall heat transfer. It is the latter, then, that must be treated in some detail.

What is uncertain from one site to another is the construction of the wall. This is important because it dictates the thermal resistance to the energy sink for the hot gases in the chamber following incineration. Two possibilities give some limiting considerations. In one, the construction could consist of a metallic or other material enclosure of specified thickness. In the other case, something like the tunnel wall or some other type of hole in the ground might represent the situation. The first of these alternatives could be treated by transient conduction through a plate, but an overall heat-transfer coefficient approximation might work in some situations. An underground cavern construction is taken here to represent the actual test situations. A similar approach to what is outlined here could be used for other types of situations.

Now consider the heat transfer into the cave wall. In essence, this enclosure is like a semi-infinite solid with convection taking

place at the surface (radiation is neglected here). A one-dimensional numerical approach can be used to represent this. Another approach, applied here, is to use a numerical method based upon an analytical solution. What is of great importance to the model is to be able to have a reasonably accurate representation of the wall temperature as a result of the heat flow into it.

Carslaw and Jaeger[7] give a solution for the transient flow of heat into a plane surface of a semi-infinite solid with a specified heat-transfer rate at the surface. This result can be combined with Duhamel's integral to allow a time-dependent heat-transfer rate from the gas to the wall. One issue to note is that the time variation of heat transfer is not really specified a priori. If, however, the integral is evaluated over a series of time steps where the heat-transfer rate is indeed found at each time step before the Duhamel calculation, this will satisfy the requirement of knowing the heat transfer prior to each calculation step.

Following the outline given in the preceding paragraph, the equation for the surface temperature is as follows:

$$T_{\text{surface}}(t) - T_{\text{surface}}(t=0) = \frac{\alpha^{\frac{1}{2}}}{k_{\text{wall}}\pi^{\frac{1}{2}}} \int_0^t \frac{\dot{Q}_{\text{wall}}(t-\tau)}{A} \frac{\mathrm{d}\tau}{\tau^{\frac{1}{2}}} \quad (5)$$

This is evaluated on a finite time-step basis as follows. At a given time, the heat transfer to the wall is assumed to be known from Newton's law of cooling.

$$\dot{Q}_{\text{wall}}(t-\tau) = \bar{h}A[T_{\text{surface}}(t-\tau) - T_{\text{chamber}}(t-\tau)] \quad (6)$$

Next, an energy balance on the tunnel gas produces

$$-\dot{Q}(t) = m_2(\Delta u_{\text{gas}}/\Delta t) \quad (7)$$

where $\Delta u_{\text{gas}} = u[T_a(t+\Delta t)] - u[T_a(t)]$. The value $\dot{Q}_{\text{wall}}(t-\tau)$ in Eq. (5) was taken outside the integral and treated as a constant for each time step (but allowed to vary at the next time step). Equation (5) could then be solved as a definite integral as shown in Eq. (8):

$$\int_a^b \tau^{-\frac{1}{2}}\,\mathrm{d}\tau = 2\sqrt{b} - 2\sqrt{a} \quad (8)$$

Equation (5) can then be rewritten as Eq. (9) with use of the constant $c \equiv \alpha^{1/2}/Ak_{\text{wall}}\pi^{1/2}$:

$$T_{\text{wall}}(t) - T_{\text{wall}}(t=0) = c\dot{Q}(\Delta\tau)\int_0^t \tau^{-\frac{1}{2}}\,\mathrm{d}\tau \quad (9)$$

Equation (9) was solved in discrete time intervals of $\Delta\tau$. The first three iterations are shown next. At the first time step, $t = \Delta\tau$ and the right-hand side of Eq. (9) reduces to

$$\dot{Q}(0)\cdot c\cdot\left(2\sqrt{\Delta\tau} - 2\sqrt{0}\right) \quad (10)$$

At $t = 2\Delta\tau$ the right-hand side of Eq. (9) becomes

$$\dot{Q}(0)\cdot c\cdot\left(2\sqrt{2\cdot\Delta\tau} - 2\sqrt{\Delta\tau}\right) + \dot{Q}(\Delta\tau)\cdot c\cdot\left(2\sqrt{\Delta\tau} - 2\sqrt{0}\right) \quad (11)$$

Similarly, at the third time step $t = 3\Delta\tau$ the right-hand side of Eq. (9) becomes

$$\dot{Q}(0)\cdot c\cdot\left(2\sqrt{3\cdot\Delta\tau} - 2\sqrt{2\cdot\Delta\tau}\right) + \dot{Q}(\Delta\tau)\cdot c$$
$$\cdot\left(2\sqrt{2\cdot\Delta\tau} - 2\sqrt{\Delta\tau}\right) + \dot{Q}(2\cdot\Delta\tau)\cdot c\cdot\left(2\sqrt{\Delta\tau} - 2\sqrt{0}\right) \quad (12)$$

These results can be generalized for the ith time step as

$$\dot{Q}(0)\cdot c\cdot\left[2\sqrt{(i)\cdot\Delta\tau} - 2\sqrt{(i-1)\cdot\Delta\tau}\right] + \dot{Q}(\Delta\tau)\cdot c$$
$$\cdot\left[2\sqrt{(i-1)\cdot\Delta\tau} - 2\sqrt{(i)\cdot\Delta\tau}\right]\ldots + \dot{Q}[(i-1)\cdot\Delta\tau]$$
$$\cdot c\cdot\left(2\sqrt{\Delta\tau} - 2\sqrt{0}\right) \quad (13)$$

The net result is that an analytical solution for the heat conduction in the (assumed) semi-infinite wall has been cast into a finite difference form to be adaptable to the energy-balance type of solution being carried out here. This can now be applied to some specific situations evaluated in tunnel tests of burning of energetic materials.

The other aspect of the analysis is estimating the heat transfer from the space to the wall. One mode could be via radiation. As just noted, this will be neglected here, assuming that the space is filled with smoke.

Another mode that will be present is convection. This could range from something quite intense while the physical burn is taking place, to something considerably more orderly near the end of the whole process. In any case, this is very difficult to predict without performing a three-dimensional analysis. We take natural convection here to be the mode of transport. For this, the natural convection is treated as though it occurs with a constant heat-transfer coefficient.

Results and Discussion

Two general categories of results can be found from the model. First, the maximum pressure and the space-averaged maximum temperature are found simply from the thermodynamics of the situation. Because these depend only on the initial condition and the amount of energy added to the chamber, the amount of energy in the fuel is a critical aspect of these calculations.

First Series of Tests

Consider the propellants used for the three cases of the first series of test. Properties of these propellants are shown in Table 1. The total energy-generated values are given in the fourth column. These are used to determine the maximum temperatures and pressures anticipated in the chamber. First consider the chamber maximum pressures (see Fig. 2).

As shown in Fig. 2, it is clear that the analytical approach overpredicts the maximum chamber pressures. This is good in that it is conservative. (Enclosures designed to tolerate the calculated maximum pressures will be of sufficient strength to tolerate the actual pressures achieved.) A quite real possibility is that the liberation of energy from the burn might not be instantaneous, as assumed here. This is felt to be the primary issue in the differences between the predicted and the measured pressures. When the temperature vs time predictions are compared to the measured values, this will again be noted. Another issue, less clear, is that the pressure gauge(s) used to measure these pressures might not have the appropriate time response.

Table 1 Propellant characteristics for the first series of tests

Case	Propellant, kg	Heat of combustion, cal/gm	Total energy Generated, J
I	680	764	2.182×10^9
II	1360	764	4.364×10^9
III	544	600	1.371×10^9

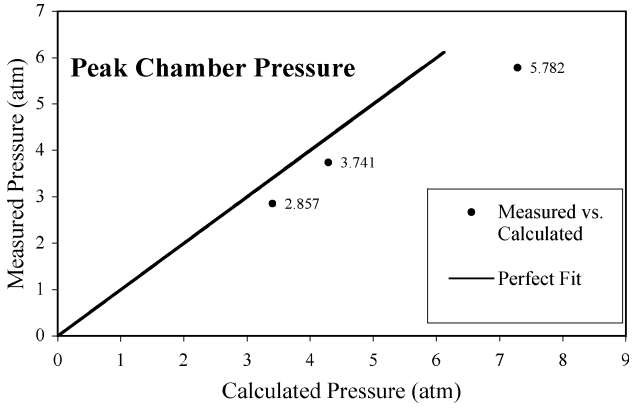

Fig. 2 Calculated vs measured maximum pressures are shown.

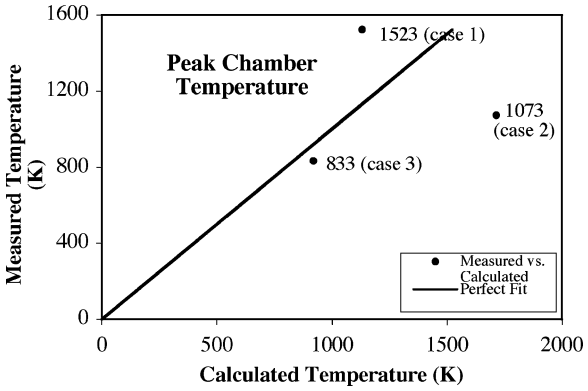

Fig. 3 Calculated vs measured peak chamber temperatures are shown. Cases refer to Table. 1

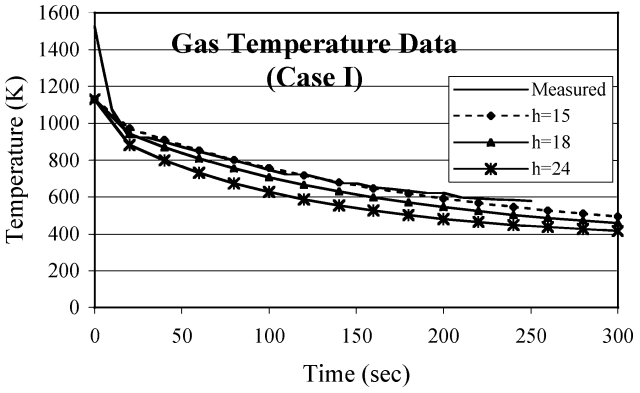

Fig. 4 Measured[8] and calculated gas temperature data for case I.

The comparisons of calculated peak temperatures with measured peak temperatures are shown in Fig. 3. Peak temperatures within the chamber are harder to correlate than are pressures. The reason for this involves the fact that the temperature varies considerably in space during and immediately after the burn process. A limited number of temperature sensors, used to measure gas values inside the chamber, will thus indicate values that vary similarly. Hence, it would not be expected that a lumped temperature approach would yield something highly comparable to measured values. As can be seen from the figure, this is indeed the case. Unlike the peak pressure correlations, the measured peak temperatures do not correlate well with the energy liberated.

Now consider the temperature vs time characteristics of the chamber. These can be used to determine the period required for the chamber to assume nearly the same temperature as was present prior to the test. Although there are many descriptive parameters required in that model that are not well known a priori to a test, the convective heat-transfer coefficient h between the gas and chamber walls is clearly one of the more critical ones. We have treated this in two ways. Both use actual test results to evaluate typical values of h to flesh out the model. In one, simply a constant value of convective heat-transfer coefficient is used. A typical value is applied to the model, and the results of the model are then compared to the measured results. Computational results can be adjusted by varying this parameter. Some examples of this are shown in Figs. 4–6. The indication of "Case" refers to the combination of parameters shown in Table 1.

In Fig. 4, the gas temperature decay with time is shown for case I. The solution to the mathematical model was carried out in time increments of $\Delta t = 20$ s for a time period of 1000 s. The first 300 s are shown to correspond to experimental data that were available.[8] Note that time $(t = 0)$ starts at the completion of the burn process when the peak gas temperature has been reached. The convection heat-transfer coefficient was varied in the range of 15–24 W/m^2 K. Values of $\bar{h} = 15$ and 18 appeared to be a fairly good match. A value of $\bar{h} = 24$ showed a definite underprediction of temperatures.

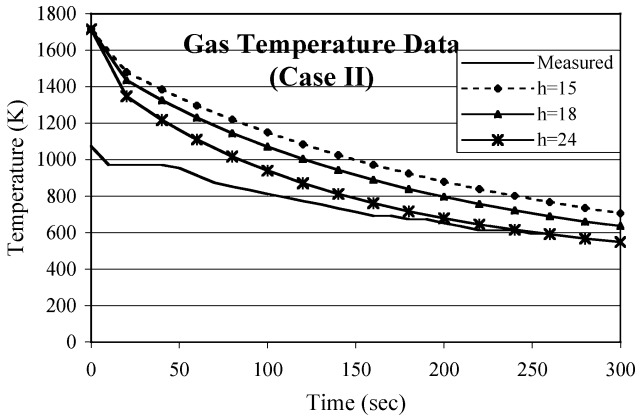

Fig. 5 Measured[8] and calculated gas temperature data for case II.

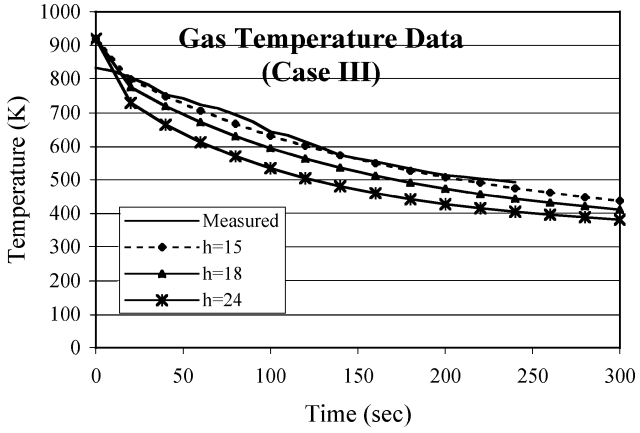

Fig. 6 Measured[8] and calculated gas temperature data for case III.

In Fig. 5, the gas temperature decay with time is shown for case II. The solution details are similar to those noted for Fig. 4. The calculated temperatures for case II suggest that higher temperatures should be expected for the measured values. Nonetheless, variations in the convection heat-transfer coefficient from 15–24 W/m^2 K produce similar results to those seen in Fig. 4.

In Fig. 6, the gas temperature decay with time is shown for case III. The solution was carried out in a similar way to those for Figs. 4 and 5. Values of $\bar{h} = 15$ and 18 appeared to be a fairly good match. A value of $\bar{h} = 24$ showed a definite underprediction.

In all cases, the temperature vs time plots show a slower rate of cooling than that predicted by the model. A problem in making direct comparisons is the variation of apparent chamber temperature at the end of the burn process as shown in Fig. 2. This value is the initial condition for the time-dependent solution, and paucity of experimental data for averaging of the chamber temperature in these early times biases the attempt at a correlation.

Second Series of Tests

A second set of data was a bit more revealing. In this situation, different energetic materials were burned (distinct from those in the first test), and many more temperature sensors were used. The latter aspect allowed the degree of data spread to be examined. In each of three cases, the same energetic material charge was used. Data for this are given here: energetic material was 199.1 kg; heat of combustion was 2712 cal/gm; total energy generated was 2.26×10^9 J; and peak temperature was 915.4 K.

In this series of tests, we estimated the heat-transfer coefficient from a natural convection correlation. Because of uncertainties about the flow situation in the cavity, a constant value of h is again assumed, but this time based upon an actual estimate. For example, the form of the predictive equation of the heat-transfer coefficient assumed for turbulent conditions is as follows:

$$\bar{h} = c(k/L)Gr^{\frac{1}{3}}Pr^{\frac{1}{3}} = ck(g\beta\Delta T\alpha/\nu)^{\frac{1}{3}} \qquad (14)$$

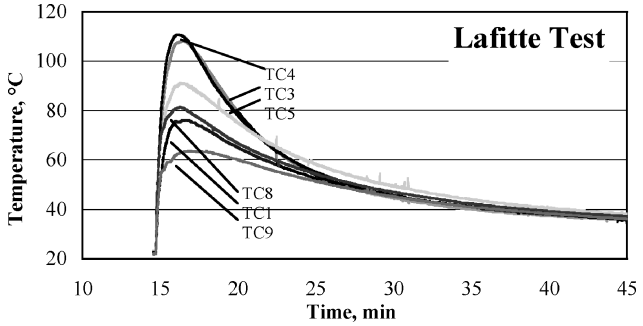

Fig. 7 Variations of the measured temperatures from the thermocouples for one of the second series of tests ("Lafitte") are shown (courtesy of B. Watkins, LLNL).

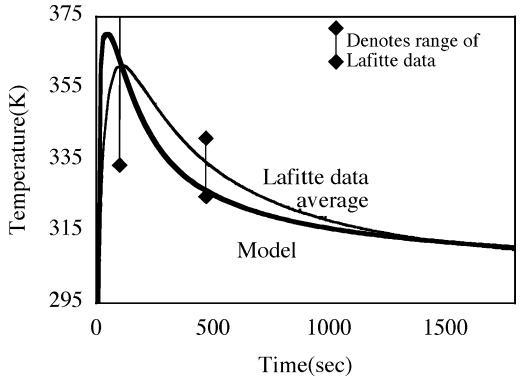

Fig. 8 Measured and calculated wall surface temperatures for the Lafitte test are shown. The bars represent the range of experimental values shown in Fig. 7.

Values for c are given for a variety of geometries. For a vertical surface, it is 0.10; and for a horizontal surface facing downward, it is 0.15; and for a horizontal surface facing upward, it is 0.27.[9] Making an arbitrary composite of these gives an overall value of approximately 0.16. For conditions represented in the second series of tests, an average value of heat-transfer coefficient was estimated to be about 36 W/m^{2}K.

Figure 7 shows a typical set of experimental data for the cavity ambient temperature response.

Figure 8 compares predicted and measured results. In this case, the experimental temperature data represent the averaged values for all temperature sensors during a test called "Lafitte." In addition to the averaged data curve, we are able to show the typical spread of experimental data from all sensors. Also shown in the figure are the predicted results using the model just described for a constant heat-transfer coefficient of 36 W/m^{2}K.

For this situation, the experimental data vary about 50% based upon the location of each sensor. With a limited number of sensors, the average of these readings is not a precise way of representing the bulk temperature in a geometrically complicated space (as was the case here). However, the model does represent the data quite well in two important aspects. First, the peak temperature predicted by the model is within 8 K of the average peak temperature. Second, the prediction of the duration of the temperature decay, which is in some senses more important for modeling purposes, is quite close. For example, in some cases, the time where the temperature had dropped to 99% of its total excursion corresponded to less than 8% difference between the model and the average of the experimental values.

Conclusions

1) A model has been proposed to predict gross pressure and temperature variations with a closed container where the burning of energetic materials is taking place.

2) The key to this model is the representation of the heat transfer to walls of the container, which is assumed ultimately to serve as the thermal sink. In the case considered here, a tunnel/cave combination made up the system for analysis.

3) Comparisons between the model and experiments show that peak pressures and temperatures during the burn are not predicted with much precision. Because the experimental data were both higher and lower than the prediction, it is clear that the complex nature of the flows within the chamber cause wide variations in the results. It is felt that the model does give a good approach to average types of variations.

4) Quite close agreement was found between the model results and the experimental results for the temperature decay time inside the container. For the case shown here, about 8% difference was found between the experiment and the model.

5) This model offers the designer of energetic material containers the ability to make a reasonable average prediction of the important parameters related to system design.

6) Other types of containers, such as metal-walled enclosures, would require a slightly different formulation of the wall heat transfer, but the general approach used here should be applicable.

Acknowledgments

The financial support of the Joint U.S. Department of Defense/Department of Energy Demilitarization Technology Program through a contract with Sandia Laboratories, Lawrence Livermore National Laboratory, and Los Alamos Scientific Laboratory (with University of Nevada, Las Vegas as a subcontractor) is greatly appreciated. Particular thanks go to Joel Lipkin, Sandia National Laboratory, and Bruce Watkins, Lawrence Livermore National Laboratory, for their excellent support.

References

[1]Hermann, H., "Disposal of Explosives from Demilitarization: A Case Study with TNT," *Combustion and Reaction Kinetics*, Fraunhofer-Inst fuer Treib und Explosivstoffe, Pfinztal-Berghausen, Germany, 1991, pp. 87.1–87.14 (in German).

[2]Zhang, L., and Wang, Z., "The State of Approach to Disposal and Utilization of Obsolete Explosives and Propellants," *Chinese Journal of Explosives and Propellants*," Vol. 21, No. 1, 1998, pp. 47–50 (in Chinese).

[3]Borcherding, R., "An Alternative to Open Burning Treatment of Solid Propellant Manufacturing Wastes," *Waste Management*, Vol. 17, No. 2/3, 1997, pp. 135–141.

[4]Martin Hughes, J., Phipps, J. F., and Sullivan, M. I., "Open Burning of Hazardous Munitions Waste," *Hazardous and Industrial Wastes—Proceedings of the Mid-Atlantic Industrial Waste Conference*, Techomic Publishing, Lancaster, PA, 1997, pp. 325–334.

[5]Vetlicky, B., and Chladek, J., "Underwater Incineration of Heterogeneous Propellants," *Journal of Propulsion and Power* Vol. 15, No. 8, 1999, pp. 925, 926.

[6]Cumming, A. S., and Paul, N. C., "Environmental Issues of Energetic Materials: A U. K. Perspective," *Waste Management*, Vol. 17, No. 2/3, 1997, pp. 129–135.

[7]Carslaw, H. S., and Jaeger, J. C., *Conduction of Heat in Solids*, 2nd ed., Oxford Univ. Press, London, 1959, p. 76.

[8]"Executive Summary of Phase II Demonstrations: The Low-Pressure Rocket Motor Burns in X-Tunnel," Dept. of Defense/Department of Energy Joint Demilitarization Technology Demonstration Program, Sandia Rept. SAND 2002-8202, Dec. 1998.

[9]Incropera, F., and DeWitt, D., *Introduction to Heat Transfer*, 4th ed., Wiley, New York, 2002, p. 513.